Radiative recombination center in As_2Se_3 as studied by optically detected magnetic resonance

J. Ristein
Fachbereich Physik der Universität Marburg, Renthof 5, D-3550 Marburg, West Germany

P. C. Taylor and W. D. Ohlsen
Department of Physics, University of Utah, Salt Lake City, Utah 84112

G. Weiser
Fachbereich Physik der Universität Marburg, Renthof 5, D-3550 Marburg, West Germany
(Received 12 April 1990)

The intrinsic luminescence of As_2Se_3 single crystals and glass has been studied by optically detected magnetic resonance (ODMR) using 16-GHz microwaves and magnetic fields up to 3 T. From these measurements we extract detailed structural information about a photoexcited center in a chalcogenide semiconductor. In the crystals a strong ODMR response is observed with the same spectral dependence as the luminescence spectrum. Resonant magnetic fields depend strongly on the orientation of the magnetic field. The measurements confirm that a self-trapped triplet exciton is the radiative state for midgap luminescence. Hyperfine splittings of the microwave transition and large zero-field splittings reveal a triplet state that is highly localized and anisotropic (almost uniaxial) with its symmetry axis oriented along a particular As—Se bond. Self-trapping of the exciton occurs at a center where lone-pair electronic states of Se interact strongly. The self-trapping leads to a redistribution of electronic charge that strengthens locally a weak intermolecular (intralayer) bond at the expense of covalent intralayer bonds. Magnetic fields enhance the luminescence efficiency, a fact that suggests the presence of a competing nonradiative recombination process, even at low temperatures, which is assumed to be related to diffusion of the self-trapped exciton. Comparison of the ODMR powder spectrum of the crystal with the ODMR spectrum of glassy As_2Se_3 indicates that similar relaxation processes also occur in amorphous As_2Se_3, where they precede at least a fraction of the recombination processes.

I. INTRODUCTION

Radiative recombination in arsenic chalcogenides is dominated by strong lattice relaxation following optical excitation. In both crystalline and amorphous samples excitation requires light of band-gap energy and leads to a broad emission band centered near the midgap position.[1] Such common behavior suggests a relaxation mechanism that arises from peculiarities of the chemical bonds rather than from native defects or impurities.

Early models invoked metastable configurations of undercoordinated and overcoordinated chalcogen atoms which are normally twofold coordinated. The remaining pair of p electrons on each chalcogen resides in a nonbonding lone-pair p orbital. These nonbonding p orbitals form the states at the top of the valence band. Charged dangling bonds,[2] C_1^+ and C_1^-, or valence alternation pairs,[3] C_1^- and C_3^+, were assumed to exist in sufficiently high concentrations to provide centers for a very efficient radiative recombination. Since the coordination of the valence alternation defects depends on the charge state, capture of optically excited carriers should lead to a lattice relaxation and to the observed Stokes shift.

Studies of the influence of high electric fields, temperature, and excitation energy on the luminescence and photoconductance of single crystals of As_2Se_3 revealed that luminescence arises from recombination of geminate pairs.[4–6] A similar result has been obtained for the midgap luminescence in trigonal Se.[7] In both crystals, it was found that at low temperatures almost all carriers excited with little excess energy recombine geminately. In crystalline As_2Se_3 the dependence of the luminescence on exciting light intensity further suggested that the radiative center is created by the excited carriers themselves forming self-trapped excitons.[8] From the long lifetime which is altered by magnetic fields of moderate strength,[9] and from the observation of an activated radiative rate of quite small activation energy (4 meV), a model of the self-trapped exciton has been proposed which envisages a spin-triplet state separated by only 4 meV from its singlet state.[8]

Based on these observations, on details of the crystal structure,[10] and on the nature of the states at the top of the valence band and at the bottom of the conduction band,[11] it has been proposed that holes are rapidly trapped in lone-pair states of Se. Each of these trapped holes creates a charged center which, on the time scale of a few picoseconds, captures an electron in a perturbed antibonding state of the local covalent bond. The trapped electron causes further alteration of the local structure and creates a relatively stable excited state with a lifetime close to 1 ms at 2 K.[12]

Although this detailed picture of the radiative center in As_2Se_3 has emerged, a crucial difficulty remains. The magnetic-resonance signatures anticipated for a triplet excitonic state have not been observed, either by LESR (light-induced electron-spin resonance) or by ODMR (optically detected magnetic resonance). Because of the failure to observe these resonances, there is no experimental confirmation of the proposed structure of the self-trapped exciton.

The present paper reports a strong and highly anisotropic ODMR signal in As_2Se_3 single crystals which provides the missing confirmation and reveals new and unusual properties for the radiative center. The spectrum of the crystalline material will also be compared to that of the glass.

II. EXPERIMENTAL DETAILS

Three different types of As_2Se_3 crystals were used, all grown from the vapor phase in a glass tube of 5 mm diameter. The source was $5N$ grade As_2Se_3 held in alumina boats at 380 °C. In order to develop a few seeds the temperature was reduced for a few hours. Crystals of different shapes grew depending mostly on the atmosphere in the tube.

Large platelets (type A) of typical size $10\times5\times0.3$ mm^3 grew in 100–200 Torr Ar with iodine added as a reactive agent. The large **a-c** faces, the cleavage planes of the crystals, are of excellent optical quality. Thicker samples (type B) of $3\times2\times1$ mm^3 size were obtained in evacuated tubes with iodine still present as a transport agent.

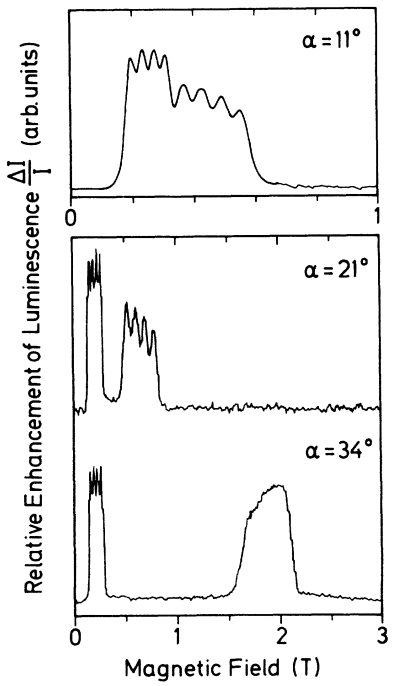

FIG. 1. ODMR spectra of c-As_2Se_3 for three different orientations of the magnetic field within the **a-b** plane of the crystal (see Fig. 6). The rotation angle α is between the field and the **a** axis. Note the different scale of the magnetic-field axes in the uppermost and the lower two spectra.

PIXE studies (proton-induced x-ray emission) failed to detect iodine in the samples, which indicates an upper limit for iodine concentration in the range of 10^{18} cm^{-3}. To exclude possible artifacts due to the presence of iodine a third type of crystal (type C) was grown in an evacuated tube where the growth mechanism depended only on the diffusion of As_2Se_3. Using this method, smaller samples (up to $3\times3\times0.2$ mm^3) of poorer surface quality were obtained in about 2 weeks. A bulk sample of amorphous As_2Se_3 was obtained by quenching from the melt, cutting, and polishing.

For all measurements the samples were immersed in superfluid He ($\sim$2 K) in a 16-GHz optical transmission cavity. Luminescence was excited by light of 2-eV energy from an actively stabilized dye laser and collected on the opposite side of the sample. For spectrally resolved measurements, the emitted light was dispersed by a 25-cm grating monochromator. At low temperatures the penetration depth of the 2-eV light is ≤ 1 μm in As_2Se_3.

ODMR measurements were performed with 500 mW microwave power chopped at 800 Hz. Luminescence was measured with a cooled Ge detector and analyzed either by a lock-in amplifier or by a digital averaging oscilloscope in the case of transient ODMR measurements. A superconducting magnet provided fields up to 3 T.

III. EXPERIMENTAL RESULTS

Figure 1 shows a typical ODMR spectrum for a type-B crystal for magnetic fields in the **a-b** plane. The three traces in this figure represent three different orientations with respect to the **a** axis (for crystal structure see Fig. 6). The spectrum consists of two clearly resolved hyperfine quadruplets. As the angle of the magnetic field with respect to the **a-c** layer plane increases, one of the quadruplets shifts rapidly to higher values of the resonant magnetic field. For $\alpha=34°$ the hyperfine structure of the high field resonance is no longer resolved.

The signal, which is surprisingly large, corresponds to a 2% enhancement of the luminescence. This large amplitude of the ODMR signal provides strong evidence that it arises from modulation of the intrinsic luminescence. Further confirmation comes from the fact that identical ODMR spectra are observed in all three types of crystals.

As an additional test, spectrally resolved ODMR measurements were performed and compared with the luminescence spectrum obtained immediately after the ODMR scan. The comparison in Fig. 2 proves that both the ODMR and the luminescence have the same spectral dependence. This fact is in contrast to the defect-related ODMR signal reported by Robins and Kastner[9] for As_2Se_3 crystals of type A. Using X-band microwaves, these authors found a very weak ODMR spectrum ($\Delta I/I\approx2\times10^{-4}$) from a luminescence peak which was shifted to lower energy by about 0.2 eV. This shift in the luminescence may be due to the presence of some iodine in the sample.

To complete the survey of the ODMR properties of the single crystals, the transient responses of the luminescence to square-wave pulses of microwave power are

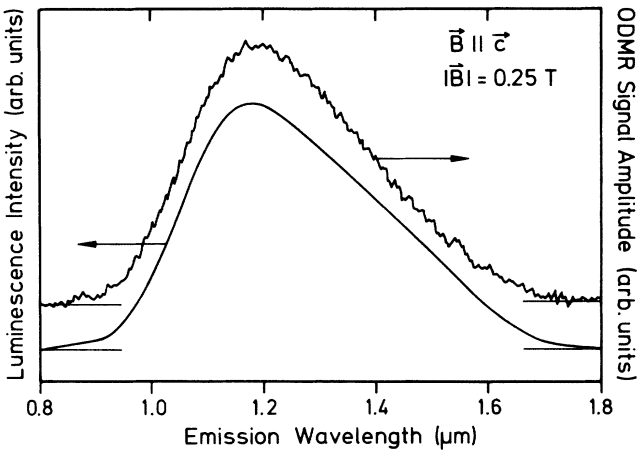

FIG. 2. Comparison between the spectrally resolved ODMR and the luminescence spectrum itself for one specific resonance condition.

shown in Fig. 3. The luminescence responds to the switching on of microwave power with a fast increase, which then decays to a new steady-state value. Such behavior is characteristic of modulation of the radiative rate. The lower trace shows a rough model calculation which reproduces some of the features of the experimental curve and is discussed in Sec. IV E.

ODMR measurements were performed for many orientations of the magnetic field both out of [Fig. 4(a)] and within [Fig. 4(b)] the **a**-**c** layer plane. Since spin-resonance conditions are invariant with respect to a sign reversal of the magnetic field, only π (180°) rotations are necessary for a complete characterization of the orientational dependence of the ODMR. For the same reason, symmetry axes in any rotation pattern necessarily have to occur pairwise, separated by $\pi/2$. Figure 4(a) shows the pattern for rotation of the field around the **c** axis; rotation around the **a** axis yields a similar pattern which is not shown here.

Rotation of the magnetic field out of the layer plane

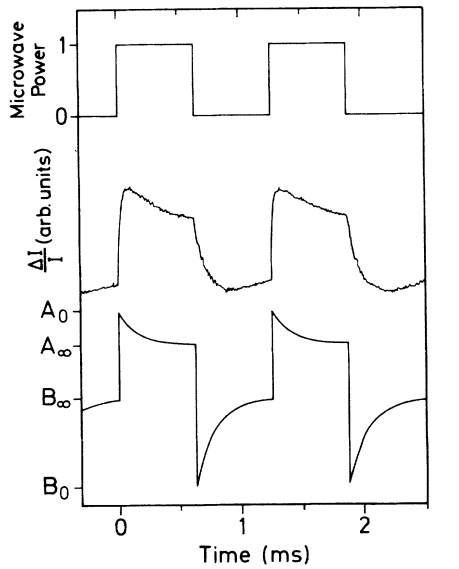

FIG. 3. Transient ODMR response (middle trace) with square pulse microwave excitation (upper trace). The resonant magnetic field was 0.63 T at an orientation within the layer plane with angles of 35° to the $-$**c** and 55° to the $+$**a** axes, respectively (see Fig. 6). Lower trace: schematic representation of the transient expected from considering a simplified rate equation for the luminescence as discussed in Sec. IV E.

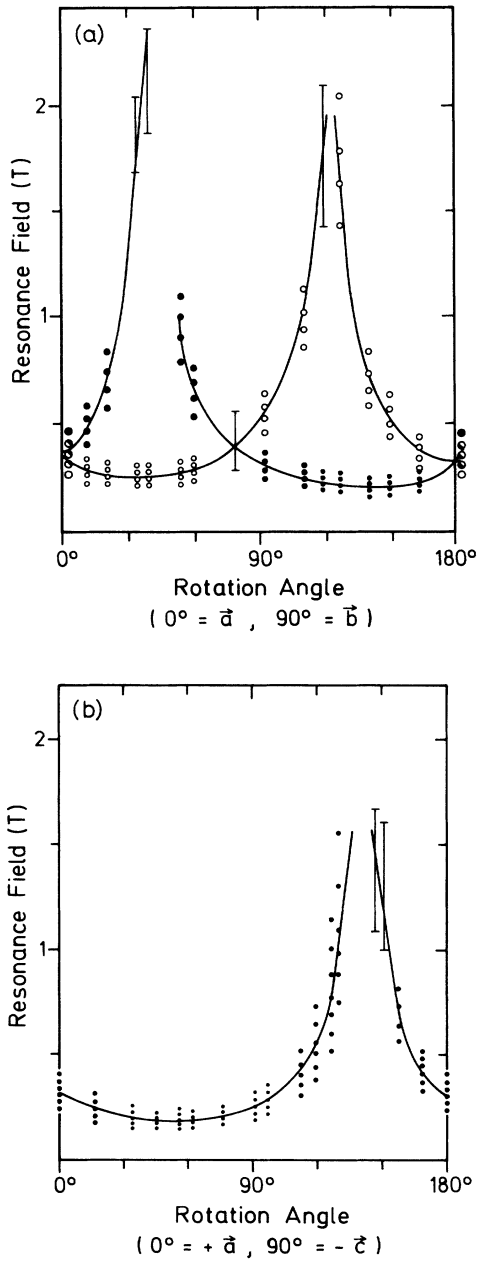

FIG. 4. Dependence of the ODMR resonances on the orientation of the magnetic field. (a) Rotation out of the layer plane around the **c** crystal axis. (b) Rotation within the layer plane around the monoclinic **b** axis. Solid curves through the average of the observed hyperfine multiplets are guides to the eye.

[Fig. 4(a)] yields two quadruplets which are only degenerate when the field is in the layer plane (**H⊥b**). The pattern is almost symmetric about the **b** axis. The deviation of that mirror symmetry from the *b* axis, which is apparent in Fig. 4(a), is due to a small tilt of the rotation axis out of the **a**-**c** plane caused by slight misalignment of the sample rotating device. In evaluating the spectra this misalignment was taken into account. The resonance shifts very rapidly with orientation of the magnetic field and shows two pronounced maxima. Close to these maxima the hyperfine quadruplet is no longer resolved, but rather the lines are smeared into a broad band whose width is indicated by bars in Fig. 4.

Rotation of the field within the layer plane, perpendicular to the **b** symmetry axis of the crystal, yields only one multiplet for all orientations [Fig. 4(b)]. This rotation pattern again exhibits a pronounced maximum in the resonant field as a function of angle. For some orientations more than four lines are observed, but this result is again due to a small misalignment of the rotation axis. The sensitivity of the degeneracy to misalignment is apparent by looking near $+\mathbf{a}$ and $-\mathbf{a}$ in Fig. 4(a). It is important to note that in contrast to the rotation pattern shown in Fig. 4(a), this rotation pattern is not symmetric with respect to the crystal axes **a** and **c**. This lack of symmetry is a consequence of the crystal symmetry and gives important hints concerning the local structure of the luminescence center. For rotation of the magnetic field within the **a**-**c** layer plane the sign of the angle with respect to the **a** axis is also important.

The ODMR spectrum of an amorphous As_2Se_3 sample is shown in Fig. 5. The well-known fatiguing effects on the luminescence in glassy chalcogenides[13] were minimized by using weak excitation of 1.5 mW and photons of large penetration depth (≥ 10 μm at 1.87 eV). Under these conditions the luminescence intensity decreased only by 10% during the scan of the magnetic field and this decrease could easily be corrected for in the evaluation. An enhancing ODMR signal is observed, which can be described by superposition of a broad 'background" signal and a pronounced $g=2$ resonance. The maximum amplitude in Fig. 5 corresponds to an enhancement of the luminescence of 0.25%.

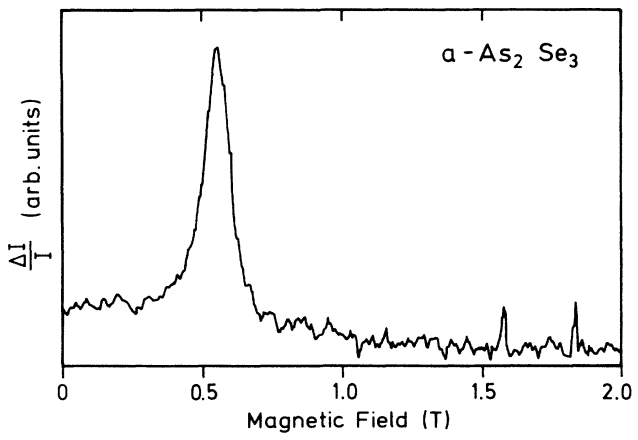

FIG. 5. ODMR spectrum of bulk glassy As_2Se_3 at 15.6 GHz. See text for details.

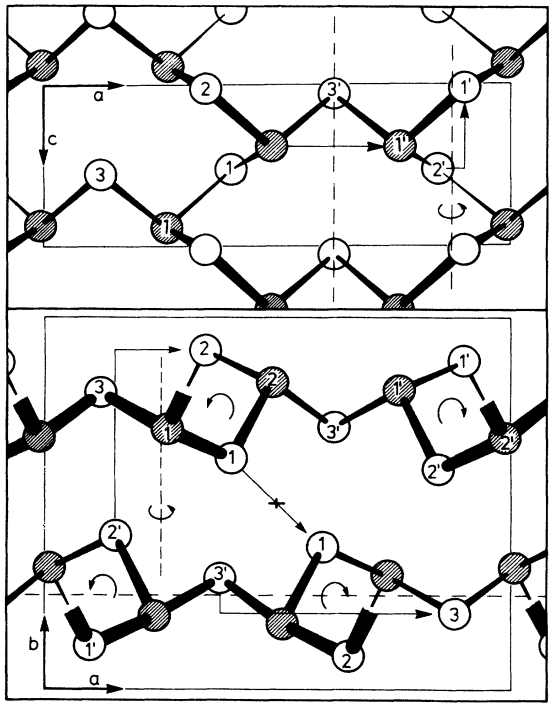

FIG. 6. Projections of the unit cell of crystalline As_2Se_3 parallel and perpendicular to the layer planes of the crystal. The nontrivial symmetry operations of the full crystal are indicated in the lower part of the figure. Different symmetry operations hold for the isolated layers and are indicated in the top part of the figure.

IV. DISCUSSION

A. Crystal symmetries of As_2Se_3

For the analysis of the ODMR we need to point out some significant features of the crystal symmetry (space group C_{2h}^5). Figure 6 shows two projections of the monoclinic unit cell which contains four As_2Se_3 molecular units. Alternating twofold-coordinated Se and threefold-coordinated As atoms form helical chains running along the **c** direction. Chains of different handedness are connected by Se bridging atoms (positions 3,3′) leading to tightly bound layers of orthorhombic symmetry. Much weaker forces hold these layers together along the **b** axis, such that each unit cell contains atoms from two layers related to each other by inversion on the center of the cell. Crystals are easily cleaved perpendicular to **b** by adhesive tape. Nevertheless, the nonbonding 4*p* electron pairs on Se_1 sites interact strongly between sites on different layers.[11]

It is an interesting and useful detail of this structure that the tightly bound layers have almost orthorhombic symmetry (C_{2v}^7) which is different from the monoclinic symmetry of the full crystal. This layer symmetry plays an important role in studies of IR and Raman-active phonons[14] and of the optical properties.[15] The symmetry of the response of a particular electronic state to an external perturbation will thus depend on the influence of the in-

terlayer interaction on that state.

The upper part of Fig. 6 shows two of the symmetry elements of the isolated layer, a screw axis $2c$ and a mirror plane $\overline{2a}$. Because of these symmetries **a** and **c** are symmetry axes of a single layer. The operations of the full crystal are shown in the lower part of Fig. 6 viewing the layers edge on. An inversion center and a twofold screw axis $2b$ interchange atoms of different layers. These operations destroy the $2c$ and $\overline{2a}$ symmetries of a single layer, so that only the other two symmetry operations, the identity and a glide plane $\overline{2b}$, survive when the layers are stacked to form the crystal. For the full crystal only the stacking axis $\overline{b}$ is an orientation of distinct symmetry.

How much of the symmetry of the single layer survives for a particular state obviously depends on the degree of its confinement to a single layer. Due to the loss of the mirror plane $\overline{2a}$ neither Se nor As sites 1 and 2 are equivalent. Indeed, band-structure calculations show that the topmost filled electronic band is derived from nonbonding p orbitals on Se (1) sites oriented almost parallel to the layer plane with amazingly little contribution from Se (2).[11] In most other aspects, however, the interlayer interaction seems to have little influence. The monoclinic angle[10] $\beta=90.5°$ is very close to $\beta=90°$ and the atomic positions in a layer deviate at most by 0.2 Å from their orthorhombic positions.

B. Symmetries of the ODMR spectrum

In this section we discuss some general aspects of the ODMR spectra beginning with the hyperfine splitting. The only stable Se isotope of nonzero nuclear spin ($I=\frac{1}{2}$), ^{77}Se, has a small natural abundance (7.6%) whereas As has one stable isotope ^{75}As whose nuclear spin is $I=\frac{3}{2}$. The hyperfine splitting of four lines is a clear fingerprint of a single As nucleus interacting with the electronic spin of the excited state, and this fact points to strong localization. If a substantial part of the wave function were extended over more than one As atom, more hyperfine lines would be seen.

Another important result is that only one magnetic resonance is observed. The two quartets of resonances shown in Fig. 4(a) are not transitions between different sublevels of a triplet state but are a consequence of crystal symmetry. Regardless of its local structure, the luminescent center will occur in two distinct orientations related to each other by the glide plane $\overline{2b}$. Therefore, resonant fields will occur pairwise, related to each other by the glide plane $\overline{2b}$, and ODMR patterns for rotating **H** around any axis perpendicular to **b** (out of the plane rotation) will be symmetric with respect to orientations parallel and perpendicular to the **b** axis, in accordance with the data in Fig. 4(a).

The other independent symmetry operation of the crystal, the inversion, provides two additional sites for the photoluminescence (PL) center. However, since inversion only corresponds to sign reversal of the magnetic field, which does not influence the magnetic-resonance conditions, no further resonances occur. The number of observed transitions thus provides no conclusive evidence for a triplet state but is compatible with either a doublet or a triplet state.

It is enlightening to consider the implications of layer-symmetry operations for the ODMR spectrum. Since the glide plane $\overline{2b}$ is both a symmetry of the layer and the full unit cell, rotation patterns for out-of-plane rotations of the field will still have the symmetry discussed above. The mirror plane $\overline{2a}$, however, will play the same role for in-plane rotation of the magnetic field, and the ODMR rotation pattern should be symmetric with respect to the **a** and **c** axes. The corresponding rotation pattern in Fig. 4(b) shows no such symmetry, indicating that the isolated layer symmetry does not hold for the self-trapped excitonic state. Obviously an interlayer interaction plays an important role in the formation of the luminescent center.

It should be mentioned that the determination of the orientation of the crystal axes in the sample under study was not a trivial task. Although the space group is clearly monoclinic, the point group is very close to orthorhombic, and the x-ray-diffraction pattern is almost invariant to rotations by π around both the **a** and **c** axes. The final determination required careful orientation of the **a**-**c** planes of a relatively thick sample perpendicular to the x-ray beam in order to distinguish the monoclinic angle $\beta=90.5°$ between **a** and **c** from its complementary angle of 89.5° between **a** and $-$**c**.

C. Spin parameters of the luminescent center

The striking dependence of the ODMR resonance on the orientation of the magnetic field points to a highly anisotropic spin Hamiltonian for the radiative center. Although much evidence points to a triplet state, only one transition has been found. Thus the possibility of an $S=\frac{1}{2}$ state of a hole and an electron with negligible exchange interaction cannot be dismissed out of hand.

The spin Hamiltonian of this latter case contains the single particle of spin **S** (in units of $\hbar$) and the external magnetic field **H**:

$$h_s=\mu_0\gamma\mathbf{H}\cdot\mathbf{g}\cdot\mathbf{S}\ , \tag{1}$$

where $\gamma=\hbar e/(2m_e)$ and μ_0 is the vacuum permeability.

Spin-orbit coupling is included in **g**, a symmetric second-rank tensor. The orientational dependence of the magnetic resonance is solely due to an anisotropy of this tensor [we ignore hyperfine interactions in Eq. (1)] which contains, besides its three diagonal elements, three nondiagonal elements that determine the orientation of its principal axes (three Eulerian angles).

For a spin triplet the dipolar interaction between the magnetic moments of an electron and a hole is not negligible with respect to the Zeeman term and this fact adds a further term to the Hamiltonian,

$$h_t=\mu_0\gamma\mathbf{H}\cdot\mathbf{g}\cdot\mathbf{S}+\mathbf{S}\cdot\mathbf{D}\cdot\mathbf{S}\ , \tag{2}$$

where **S** is the total spin operator of the electron and hole. **D** is a traceless symmetric tensor with elements

$$\mathbf{D}_{ij}=\frac{\mu_0(\gamma g_{\mathrm{el}})^2}{(8\pi)}\left\langle\frac{r^2\delta_{ij}-3x_ix_j}{r^5}\right\rangle\ ,$$

where $g_{el} \approx 2$ is the g factor of the free electron and the angular brackets indicate averaging over the spatial part of the two-particle wave function. The coordinate $\mathbf{r} = \mathbf{r}_e - \mathbf{r}_h$ is the relative one between the electron and the hole.[16] In both Eqs. (1) and (2) we have ignored the hyperfine interaction between the electronic and nuclear spins.

A second contribution to this spin-spin interaction term arises from the spin-orbit interaction taken to second order. In hydrocarbons the spin-orbit interaction accounts for contributions to the magnitude of D ranging from 3×10^{-4} GHz in the benzene radical[17] to 3 GHz in the linear CH_2 radical.[18] The free-atom spin-orbit coupling constants for As and Se are somewhat more than 50 times larger than that of C.[19] Since the contribution to D goes as the square of the coupling constant it can be seen that very significant splittings can arise from this source. We discuss this situation in more detail below.

We assume identical orientations of the principal axes of g and D both of which are related to the local symmetry of the radiative center. The tensor D is then uniquely characterized by the splitting of the three magnetic sublevels in zero magnetic field. Because D is traceless, one can describe this tensor in its principal axis system by two independent parameters D and E. According to the usual definition $2 \cdot E$ is the splitting of the closest two levels at zero field, and D gives the separation of the third one from the average of the other two.

The parameters of the Hamiltonians (1) and (2) were determined from a fit to the average position of the observed quadruplets in the three ODMR rotation patterns (solid lines in Fig. 4). The hyperfine interaction was not included. The results are summarized in Table I.

In the triplet model we must assume that microwave transitions are observed only between the two sublevels which are closest in energy. The zero-field splitting of these two levels $2 \cdot E$ (12.4 GHz) is determined quite accurately because the resonant field at the flat part of the rotation pattern depends critically on this value. The pronounced orientational dependence of the ODMR resonant fields results from a large anisotropy of the radiative center, which leads to a large value of D. Since part of the anisotropy may be due to the g tensor we can give only a range of D values. We assume g to be a uniaxial tensor with its symmetry axis parallel to that principal axis of D which is associated with the third, widely separated triplet level. (If the magnetic field is parallel to a principal axis of D, the corresponding triplet sublevel does not shift with the field.) We further assume $g_\parallel = 2.0$ and examine the range of $g_\perp$ between 1.0 and 2.0. Values of D/h between 190 GHz for $g_\perp = 1.0$ and 550 GHz for $g_\perp = 2.0$ give satisfactory agreement. These values are lower limits, since larger values of D do not affect the quality of the fits significantly. These large values for E and D may appear at first glance to provide the arguments against the triplet explanation, but as mentioned above, the second-order spin-orbit contributions can, in principle, be quite large for As and Se. In fact, one might expect similarly large values for other chalcogenide crystals.

TABLE I. Eulerian angles of the principal axes system. Spin parameters of the luminescent center are determined from fits to the orientational dependence of the ODMR spectra. Eulerian angles (using the convention employed in Ref. 29) define the rotation of the crystal axes ($\mathbf{c} = \mathbf{x}$, $\mathbf{a} = \mathbf{y}$, $\mathbf{b} = \mathbf{z}$) onto the principal axes system ($\mathbf{x}', \mathbf{y}', \mathbf{z}'$) of the luminescent center. The orientation of both symmetry-related sites is listed.

Site 1	$\theta = 62°$	$\varphi = 220°$	$\psi = 200 \pm 15°$
Site 2	$\theta = 118°$	$\varphi = 220°$	$\psi = 160 \pm 15°$
$S = 1$	$E/h = 6.2$ GHz		$g_\parallel = 2.0$ (assumed)
	$D/h \geq 190$ GHz		for $g_\perp = 1.0$
	$D/h \geq 550$ GHz		for $g_\perp = 2.0$
$S = \frac{1}{2}$			$g_\parallel = 6.0$
			$g_\perp = 0.5$

Even with an anisotropic g tensor, the large ratio of $D/2E \geq 15$ points to a very anisotropic luminescent center of approximately uniaxial character. The orientation of the symmetry axis z of the D tensor is quite accurately determined from the positions of the steep maxima in the ODMR rotation patterns. With our convention of Eulerian angles, θ in Table I is just the polar angle of this z axis with respect to the $+\mathbf{b}$ crystal axis, whereas φ is its azimuth with respect to $-\mathbf{a}$.

Maxima in the rotation patterns occur when the magnetic field vector crosses the x-y plane of the D tensor, which occurs at $\varphi - \pi/2$ (with respect to a) for the rotation in the a-c plane shown in Fig. 4(b). While φ can be extracted directly from that rotation pattern, θ is determined from the rotations out of the a-c plane in a slightly more complicated way. The orientation around the z axis of the x and y axes only influences the height of the maxima of the resonant magnetic fields in the rotation patterns. The fit is not very sensitive to the orientation of these axes, so that the third Eulerian angle ψ is less accurately defined by the experiments. The orientations of the z axes of the D tensors of the two sites per unit cell are found to be within 10° of the 1—1 and 1′—1′ bonds of Fig. 6.

A model based on an $S = \frac{1}{2}$ state can also describe the observed orientational dependence of the ODMR resonances but yields a uniaxial g tensor of rather unlikely components $g_\perp = 0.5$ and $g_\parallel = 6.0$. This in itself may be considered as an argument against such a center. Further support for a triplet state comes from the dependence of the ODMR resonant field on the microwave frequency (Fig. 7). For these measurements the magnetic field was oriented such that both hyperfine quadruplets were observed. By dielectrically loading the microwave cavity, the resonant frequency could be varied by about 3%, and the corresponding shift of the magnetic field was determined. Kramer's degeneracy prohibits zero-field level splitting of an $S = \frac{1}{2}$ center and also demands that the slope $d\nu/dB$ of the lines in Fig. 7 be given by the ratio of ν_0/B_0. This dependence is indicated by the dashed lines in Fig. 7, whose obvious disagreement with the experimental data rules out an $S = \frac{1}{2}$ luminescent center.

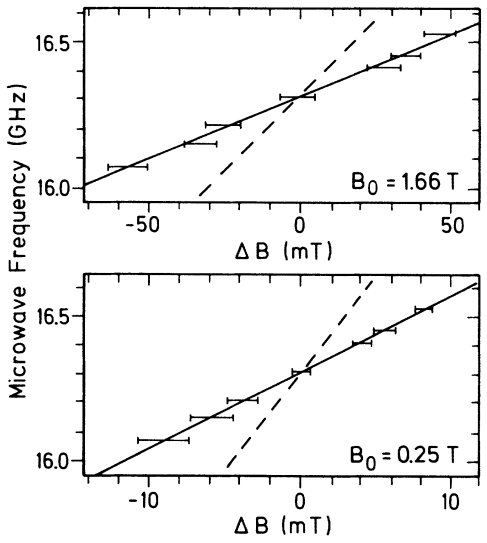

FIG. 7. Shift of the ODMR resonances with changing microwave frequency. The orientation of the magnetic field was chosen such that two quadruplets could be observed simultaneously at different magnetic fields.

The slopes of the lines through the experimental points are 4.3 and 26 GHz/T for the high-field and low-field resonances, respectively, less than half the value expected for an $S=\frac{1}{2}$ center. These values, however, strongly support the triplet state, which predicts from the parameters in Table I slopes of 4.3 and 25 GHz/T, respectively.

The ODMR results unambiguously confirm the triplet character of the radiative center and also explain the failure to find these resonances in preceding attempts. The preceding experiments were performed with X-band spectrometers employing microwave frequencies of ≈ 9.2 GHz, less than the zero-field splitting of the closest triplet levels (12.4 GHz). ODMR experiments thus could have succeeded only for orientations of the field near level crossing conditions. The parameters derived here indicate that resonance employing 9.2-GHz microwaves is possible only in 1.2% of the full 4π solid angle. Even in this case, fields exceeding 1.6 T are required to achieve resonance.

It should be mentioned that, from the dependence of the radiative decay on magnetic field, Robins and Kastner also derived an orientation of the principal axes of the radiative center.[9] Since the decay rates depend in a complicated way on the mixing of the various sublevels by the magnetic field, it is not clear how the dependence of decay rates on field orientation is related to that of the ODMR resonance. If we assume that a small influence of the field on the decay kinetics corresponds to high-field resonances in ODMR, then the patterns of Robins and Kastner are consistent with the data summarized in Table I.

The large zero-field splittings and the presence of a hyperfine quadruplet indicate strong localization of the self-trapped exciton. The zero-field splittings are an order of magnitude larger than those reported for organic molecules, but as mentioned above this difference could be due to second-order spin-orbit contributions which become larger for the heavier elements. In naphthalene, which is a π electron system extending over two benzene rings, values of $D/h=3.0$ GHz and $E/h=0.41$ GHz are reported.[16] In crystalline quartz, triplet excitons have been observed[20] by ODMR with $D/h=22.6$ GHz and $E/h=1.6$ GHz. These values are an order of magnitude greater than those found in halide crystals[21] or in typical organic molecules.[16] This trend is consistent with the very large values for D and E found in As_2Se_3, especially if the major contribution to the interaction is of the second-order, spin-orbit type. The self-trapped exciton in As_2Se_3 obviously is much smaller than the size of a naphthalene molecule. The exchange interaction then is also expected to be larger. The singlet triplet splitting $\Delta=1.8$ eV found in naphthalene[16] therefore can be considered as a lower limit for the corresponding splitting in As_2Se_3, and we expect that the singlet state of the radiative center lies in the conduction band and has no influence on the recombination kinetics.

D. Decay kinetics of the luminescence

Between 6 and 80 K, time-resolved luminescence studies of Robins and Kastner[8] show a decay rate $\nu(T)$ which is a superposition of a temperature-independent and a thermally activated contribution: $\nu(T)=\bar{\nu}+\nu_0\exp(-W/kT)$, with $\bar{\nu}=3.3$ kHz, $\nu_0=180$ kHz, and $W=4$ meV for As_2Se_3. The parameter $\bar{\nu}$ was interpreted as the average recombination rate from the excited triplet states to the ground singlet state, and $\nu_0\exp(-W/kT)$ was associated with phonon-assisted tunneling into the excited singlet state, from which fast recombination was assumed with a rate of 10^8 s^{-1}, typical for a dipole-allowed transition.[8]

There are a number of problems with this interpretation. First, since no fast initial decay was observed one had to assume, with no physical motivation, that excitation exclusively occurs into the triplet excited states. Second, the preexponential factor of 180 kHz is amazingly small. In addition, between 4 and 2 K a transition occurs from a single exponential decay with time constant $\bar{\nu}$ to a biexponential decay with $\nu_1=1.6$ kHz and $\nu_2=5.6$ kHz. The quantum efficiency in the slower component is 0.45.[9] If three triplet levels, two with decay rates too close to be resolved, gave rise to that behavior, then the value for the quantum efficiency would be expected to be close to $\frac{1}{3}$ or $\frac{2}{3}$ instead of $\frac{1}{2}$. As pointed out by Robins and Kastner,[9] this argument against the model may not be definitive because spin-lattice relaxation will tend to increase this efficiency. Finally, in light of the present ODMR results, the activation energy of 4 meV is far too low for the exchange splitting of the singlet and triplet states, but instead probably corresponds to the energy splitting of the third triplet level from the other two.

We propose an alternative interpretation, in which radiative decay occurs only out of three triplet states with decay rates of $\nu_1=1.6$ kHz, $\nu_2=5.6$ kHz, and $\nu_3=180$

kHz, respectively. Due to the large splitting of the third triplet level from the other two, spin-orbit coupling to higher-lying singlet states may be considerably stronger and thus lead to a higher recombination rate for this level. Since the mutual splitting of the other two levels is only 0.05 meV [(h)12.4 GHz], which is an energy at which there exists a very low density of acoustic phonons, cross relaxation between these two states is negligible within the optical lifetimes. This fact is directly confirmed by the transient ODMR results (see Sec. IV E).

The activation energy from the temperature dependence of the decay rate ($W=4$ meV) is the splitting of the third level from the other two, for which we could only estimate a lower limit from the ODMR data. This energy corresponds exactly to one of the rigid-layer vibrational modes of the crystal (32.5 cm^{-1}) as obtained from Raman spectroscopy.[22] We therefore assume fast cross relaxation between the third highest-lying triplet level and the other two with rates m and $m\exp(-W/kT)$ for emission and absorption of phonons. For simplicity these rates are assumed to be equal for both levels 1 and 2. Two temperature regimes have to be considered. In the first regime where $m\exp(-W/kT)\gg\nu_1,\nu_2$, all three triplet levels are in thermal equilibrium, and the luminescence decays exponentially with rate $\nu(T)=[\nu_1+\nu_2+\nu_3\exp(-W/kT)]/[2+\exp(-W/kt)]$. The denominator in this expression only varies between 2 and 3, and this formula fits the experimental data[8] above 6 K as accurately as the expression proposed by Robins and Kastner [$\nu(T)=\bar{\nu}+\nu_0\exp(-E/kT)$]. In our interpretation, however, the pre-exponential factor is no longer an attempt to escape frequency for activation into a faster decaying state, but is the decay rate out of this state. The transition to a biexponential decay, which is experimentally observed between 2 and 4 K, is the transition into the second temperature regime where $m\exp(-W/kT)\ll\nu_1,\nu_2$. In this regime, the triplet levels 1 and 2 are no longer coupled after initial population, since transitions between them via level 3 are no longer possible. As long as $m\gg\nu_3$ holds, however, generation may very well be equal into all three triplet levels without any fast recombination occurring from level 3. In this case, luminescence decays independently from levels 1 and 2, and an equal quantum efficiency of $\frac{1}{2}$ is expected in both the fast and slow components with rates ν_2 and ν_1, respectively. This behavior is observed experimentally.[8]

The only constraints on this interpretation are with respect to the rate coefficient m for cross relaxation between level 3 and levels 1 and 2. The conditions $m\gg\nu_3$, $m\exp(-W/kT)\ll\nu_1,\nu_2$ for $T\leq 2$ K, and $m\exp(-W/kT)\gg\nu_1,\nu_2$ for $T\geq 4$ K have to be fulfilled simultaneously, which leaves a range between 10^9 and 10^{13} Hz for m. If m is assumed to be 10^{12} Hz, which is the frequency corresponding to the rigid-layer mode at 32.5 cm^{-1}, then a sharp transition of the luminescence decay from exponential to biexponential is predicted at 2.5 K. On the other hand, a large value of m will lead to lifetime broadening for any transition originating from level 3, and this consideration will narrow the range of possible values for m.

E. Transient ODMR response

The behavior of the transient ODMR response in Fig. 3 can be understood with a simple model which considers the population of self-trapped excitons n and competing radiative and nonradiative rates ν_r and ν_{nr}, respectively. In this case

$$\frac{dn}{dv}=g-(\nu_r+\nu_{nr})n\ , \tag{3}$$

where g is the generation rate. The steady-state density of excited states

$$n=\frac{g}{(\nu_r+\nu_{nr})} \tag{4}$$

and the quantum efficiency of the luminescence

$$\eta_r=\frac{\nu_r}{(\nu_r+\nu_{nr})} \tag{5}$$

are altered by the incident microwaves which enhance the cross relaxation rate between the magnetic sublevels. The average radiative and nonradiative rates are changed by $\delta\nu_r$ and $\delta\nu_{nr}$, respectively. Due to the high microwave power used in the ODMR experiments, we assume that saturation of microwave transitions, and hence any change of the recombination rates, occurs fast in comparison to the lifetime $(\nu_r+\nu_{nr})^{-1}$ of the excited states.

The ODMR transient in Fig. 3 exhibits a fast increase of the amplitude immediately after switching on the microwaves,

$$A_0=\frac{\Delta I}{I(t=t_{on})}=\frac{\delta\nu_r}{\delta\nu_{nr}}\ . \tag{6}$$

This transient then decays exponentially with the new lifetime (new time constant) to a new steady state characterized by the modified rates $\nu_r+\delta\nu_r$ and $\nu_{nr}+\delta\nu_{nr}$. The steady-state change in amplitude is given by

$$A_\infty=\frac{\Delta I}{I(t\to\infty)}=\xi(1-\eta_r)\left[\frac{\delta\nu_r}{\nu_r}-\frac{\delta\nu_{nr}}{\nu_{nr}}\right]\ . \tag{7}$$

Switching off the microwaves restores the old coefficients ν_{nr} and ν_r which, in the case where the spin lattice relaxation time is short in comparison to the lifetime of the excited state, yields a fast negative spike

$$\xi=1+\frac{(\delta\nu_r+\delta\nu_{nr})}{(\nu_r+\nu_{nr})}\approx 1$$

of amplitude

$$B=\frac{\Delta I}{I(t=t_{off})}=-\xi\frac{(\delta\nu_r+\delta\nu_{nr})}{(\nu_r+\nu_{nr})}\ , \tag{8}$$

followed by an exponential approach to the initial steady state. A schematic representation of this sequence is shown as the bottom trace in Fig. 3. In the experimental trace the negative spike is smeared out, a behavior which is expected if the lattice relaxation time is comparable to, or larger than, the lifetime of the excited state. In the

limit of slow spin lattice relaxation, the return of the system to equilibrium is governed by the competing processes, decay and optical reexcitation. The transient ODMR is characterized by a decrease of the luminescence with a time constant which corresponds to the faster-decaying level followed by a subsequent increase with the slower rate. This behavior is discussed in detail in Ref. 9. By comparing the model with the experimental behavior shown in Fig. 3, it is obvious that in As_2Se_3 crystals spin lattice relaxation between the two magnetic sublevels occurs on a time scale similar to, or slower than, the triplet lifetime. An average lifetime of these two sublevels of $\tau=0.3$ ms is estimated from the transient in Fig. 3. This estimate is consistent with the results of the luminescence decay experiments.[9]

The transient ODMR also suggests the presence of competing nonradiative recombination of self-trapped excitons even at 2 K. Although the microwave pulse repetition rate of 800 Hz was too fast to reach saturation in the on and off states, it is obvious that the two limits are different, a fact that requires the presence of nonradiative processes. If we assume that the microwaves alter only the radiative rate, then from A_0 and A_∞ we can derive an upper limit for the quantum efficiency of the luminescence of $\eta_r=0.7$. Even more convincing is the result from true continuous-wave (cw) luminescence measurements in a magnetic field (Fig. 8). For an exciting wavelength near the peak of the excitation spectrum and for intensities well within the limits of the linear relationship between excitation and emission intensities, the relative luminescence efficiency is maximum. Even in this case, the luminescence excited with steady-state light and monitored by the dc output of a Ge detector increases in an external magnetic field. The luminescence monitored in this fashion approaches saturation for fields above 1 T with an increase of about 7%. An enhancement of the average radiative rate due to mixing of the triplet sublevels by the magnetic field[9] can account for this increase, but this explanation requires a competing nonradiative process.

F. Microscopic structure of the luminescent center in c-As_2Se_3

Based on results of band-structure calculations[11] that the highest-filled states are derived from nonbonding Se 4p orbitals (lone pairs) and on electric-field-modulated optical spectra which indicate considerable dispersion of the top valence-band states along the stacking axis **b**, we[23] have previously proposed a strong π-type interaction of Se 4p lone-pair states between Se (1) sites in neighboring layers across the inversion center.[12] Due to this inversion symmetry the 4p orbitals of Se (1) atoms are parallel to each other but almost orthogonal to the 4p states at Se (2) sites. The larger interaction between Se (1) states may cause large π-π^* splittings which, since all states are occupied, contribute nothing to first order to the π bonding between the layers. The π^* state, however, is pushed up and forms the top of the valence band. The π interaction provides the basis for the inequivalence of Se (1) and Se (2) atoms in the crystal. The distance between Se (1) sites is only 3.3 Å. This distance is less than the van der Waals radius of 3.6 Å, which is approximately the distance between Se (1) and Se (2′) sites in neighboring layers. The distance between Se (2) sites across the stacking axis, whose lone-pair orbitals are also parallel, is 4.1 Å.

We assume that a hole created by optical excitation thermalizes into the highest-filled states, a π^* state at Se (1) sites. This event reduces locally the repulsive electron density. As a consequence, Se (1) atoms may approach each other and enhance their π interaction, thereby weakening the σ bonds to As (1) and As (2) sites. This first step in the lattice relaxation increases the π-π^* splitting (the interlayer bond) but reduces the σ-σ^* splitting of the strong intralayer bonds. It is further possible that this relaxation pushes the local π^* state above the valence-band edge, which traps and localizes the hole immediately after thermalization. An empty σ^* state at this Se (1) site (these states form the bottom of the conduction band) may also be shifted below the conduction-band edge due to the reduced σ-σ^* splitting of at least one of the As bonds of the Se (1) atoms. This shift would provide a trap for the electron. Capture of an electron in this antibonding state will weaken that particular bond and allow further lattice relaxation at that site. This relaxation would move both electron and hole states deeper into the gap and form the self-trapped excitonic state which is the radiative center.

We now address the question of whether or not the lattice relaxation maintains the local inversion symmetry by spreading both the electron and hole wave functions over both layers equally. This situation is clearly overruled by the ODMR results, which show that only one As nucleus is seen in the hyperfine interaction, not two, as is necessary for the conservation of inversion symmetry. The formation of the self-trapped exciton spontaneously breaks the inversion symmetry, probably by capturing the electron in an antibonding σ^* state. The relaxation leads to a highly localized triplet state with a large zero-field splitting between sublevels.

The orientations of the three D tensor principal axes support this model. The axial symmetry coincides within 10° with the orientation of the Se (1)-As (1) bond direction (Fig. 6), a fact which unambiguously confirms the unique role of Se (1) sites and their inequivalence to Se (2) sites. In addition, the results show that by stacking the orthorhombic layers in the monoclinic crystal, the As (1)

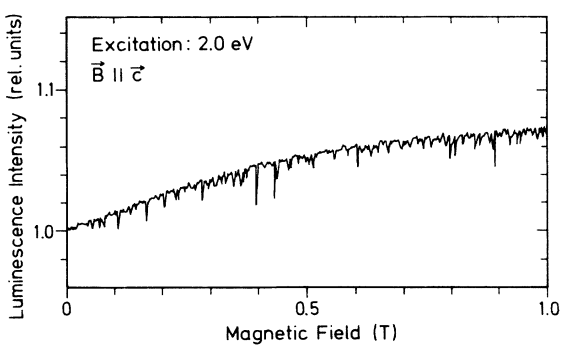

FIG. 8. True cw measurements of the change of the luminescence in c-As_2Se_3 in an external magnetic field. See text for details.

and As (2) sites also become inequivalent with the larger distortion apparently occurring in the Se (1)—As (1) bond. In this model the self-trapped exciton turns out to be a redistribution of bonding charge from intralayer bonds to interlayer bonds. Interlayer bonds become stronger as the hole reduces the repulsive electronic charge in π^* orbitals while the electron, which is simultaneously created, weakens an intralayer bond by occupying an antibonding state at the same Se (1) site. The weakening of σ bonds by electrons in an antibonding state σ^* has also been suggested in a recent calculation of threefold-coordinated Se, which is an antisite defect in *c*-As_2Se_3.[24] Occupation of the σ^* state of Se_3^+ by an electron leads to a Se_3^0 center, which stretches the bond length from 2.35 to 2.55 Å and gains a small amount of energy of about 0.1 eV.

The only significant feature of the ODMR spin Hamiltonian which is hard to reconcile with the proposed model is the large magnitude of the ^{75}As hyperfine coupling constant in the high-field regions (along the direction of the axial symmetry). The large size of the hyperfine splitting ($A \approx 0.2$ T) requires a very large As 4*s*-state contribution to the wave function of the paramagnetic electrons. The contribution of As 4*p* states can be neglected, since such a state produces only about $\frac{1}{20}$ the hyperfine splitting of a 4*s* state. The anisotropy of the hyperfine splitting is caused by the field dependence of this splitting when the Zeeman splitting and spin-spin splittings are of comparable size.[16] Since the lone-pair 4*p* states of the Se atom are essentially orthogonal to the As *s* states, the hole state should make a negligible contribution to this splitting. In the high-field limit, the triplet hyperfine splitting should be one-half that of a free ion with the same amount of 4*s* wave function. The poorly resolved splittings seen at high field are indicative of almost pure-4*s* character for the electron part of the wave function. This fact appears to be inconsistent with the known *s* and *p* character of the As-Se σ^* state.

The crystal structure also gives a hint concerning the competing nonradiative recombination of the self-trapped excitons at temperatures at low as 2 K. Luminescence efficiencies under intense excitation point to the onset of bimolecular exciton annihilation at a mean distance of about 100 Å.[12] This distance is well above the size of the self-trapped excitonic state and suggests some mobility of these excitons. The possibility of a mobile state seems to contradict the term self-trapping. However, since the trapping center is intrinsic to the crystal, equivalent sites occur in each unit cell. The strong localization of the excitonic wave function will certainly reduce the transfer-matrix element, but along the c axis the next equivalent center is only 4.3 Å away. A very small mobility of the self-trapped exciton is sufficient to explain bimolecular recombination over 100 Å. To travel that distance in the exciton's lifetime of 0.3 ms, a transfer time of 12 μs to the next unit cell is sufficient. This transfer time corresponds to a diffusion coefficient of 1.5×10^{-10} cm^2/s. This value is five orders of magnitude smaller than the diffusion coefficient at room temperature of 3×10^{-5} cm^2/s for the more extended triplet excitons in naphthalene.[25]

A second possibility to explain bimolecular exciton annihilation is an Auger process which occurs via a dipole-dipole interaction between two excitons. This process would not require the excitons to be mobile.

G. ODMR in *a*-As_2Se_3

The ODMR spectrum of glassy As_2Se_3 at 15.6 GHz (Fig. 5) is very similar to spectra reported by Depinna and Cavenett[22] and by Robins and Kastner[9] at 9 GHz. The sharp resonance at $g=2$ is attributed to distant pair recombination of electrons and holes. The linewidth of 100 mT is considerably less than that anticipated by scaling the values in the range of 80–95 mT reported in the 9-GHz experiments. This fact indicates that unresolved hyperfine interactions probably contribute to the line broadening.

The broad background, which extends up to 1.5 T, has also been observed at 9 GHz and has been interpreted as due to recombination of excitons.[9,26] From the data obtained for excitons in single crystals (Table I) we have calculated a powder spectrum of the ODMR signal. This powder spectrum reproduces the broad-background spectrum of the glass quite well (dashed line in Fig. 9). Distributions in the spin-Hamiltonian parameters will further broaden the calculated ODMR powder spectrum. Because of the large value of *D*, microwave transitions will occur only between the two triplet levels which are closest. An assumed spreading of these two levels, whose splitting is given by $2\cdot E$, will affect the ODMR spectrum the most. The lower curve in Fig. 9 shows a powder spectrum of the ODMR with a smaller value of $E/h=1$

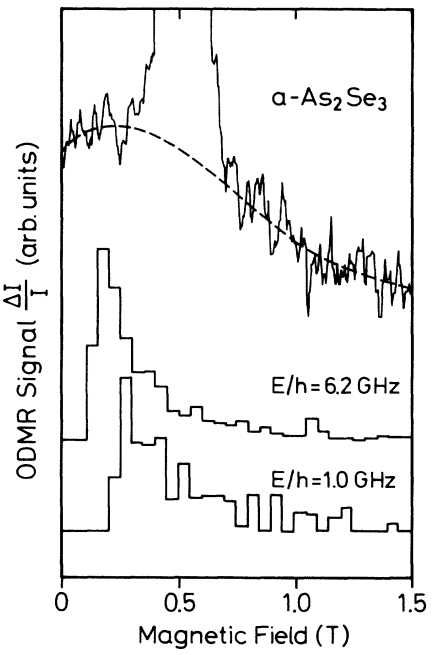

FIG. 9. Comparison of the broad ODMR background signal of *a*-As_2Se_3 with powder spectra obtained by averaging over the orientational dependence of the crystalline luminescence center. To indicate the influence of a distribution in spin-Hamiltonian parameters calculations for two different *E* values are shown.

GHz. This value generates a larger tail at high magnetic fields. The favorable comparison of the powder spectra to the ODMR response in the glass suggests that self-trapped triplet excitons also contribute to luminescence in the glass. A distribution of values of E would account for the observation of this signal in the 9-GHz experiments.

The microscopic model for the formation of self-trapped excitons rests on the combination of the lone-pair π interaction and the weakening of the σ bonds. The inversion symmetry of the crystal guarantees proper alignment of $4p$ orbitals of neighboring Se atoms. The likelihood for proper alignment in the glass is certainly much smaller, a fact which is compatible with the smaller luminescence efficiency in the glass. It is possible, however, that lattice relaxation which may be easier in the glass tends to produce the proper alignment of the $4p$ orbitals. In the glass the probability for self-trapping of holes is also reduced. In the crystal this self-trapping seems unavoidable, a fact which may explain why charge transport in the glass occurs by holes,[27] while in the crystal holes are immobile and charge transport occurs only by electrons.[28]

V. CONCLUSIONS

The present study confirms that in crystalline As_2Se_3 radiative decay of optical excitation occurs by recombination only after self-trapping of an electron-hole pair to form a triplet excitonic state with considerable reconstruction of the local bonds. (We note that with the parameters suggested for As_2Se_3 the singlet state would be above the free-exciton level and therefore unstable.) We have argued that this reconstruction is initiated by trapping of the hole at an inversion center where lone-pair $4p$ states of Se atoms strongly interact and lead to a partial π bond between atoms on different layers. This interaction weakens one of the two covalent As—Se bonds at the trapping site. Trapping of the electron in the antibonding state σ^* of this weakened bond causes further relaxation. In the relaxed excited state the weaker interlayer (intermolecular) bonds become stronger at the expense of the intralayer (intramolecular) bonds.

The self-trapped state has a number of unusual properties. A large zero-field splitting and a hyperfine splitting of the ODMR spectrum into a quadruplet reveals a highly localized center which encompasses only one As atom. This center is extremely anisotropic and almost uniaxial with its symmetry axis oriented approximately parallel to the distorted Se—As bond.

The ODMR occurs as a result of transitions between only two levels with 12.4-GHz zero-field splitting. The third level is separated by at least 190 GHz, which causes a dramatic dependence of the ODMR resonance on the orientation of the magnetic field. In the case of a symmetric g tensor this splitting increases to at least 550 GHz (2.3 meV). Thermal excitation into this level may be the reason for an activated behavior (4-meV activation energy) of the radiative decay at low temperatures. We have ruled out an alternative interpretation of this activated process as due to a thermal transition from a triplet to a singlet excitonic state. This alternative interpretation is ruled out because of the high degree of localization of the triplet excitonic state, a fact which leads to a much larger splitting of the singlet and triplet states.

Magnetic fields enhance the luminescence efficiency and reveal the presence of nonradiative recombination even at the lowest temperatures (2 K). This nonradiative recombination probably occurs by a bimolecular process which either requires some diffusion of the self-trapped state or an Auger process between two excitons. If the exciton is mobile, then the mobility is attributed to the fact that the self-trapped state is translationally invariant and to the fact that the lattice constant along the c axis of the lattice is small.

Although the relaxation of optical excitation in the crystal occurs at the inversion center, this relaxation only makes use of strong intermolecular coupling of Se lone-pair states. Sites of similar coupling should be present in disordered samples as well, though not as frequently and with some distribution of the energies involved. A broad-background signal which occurs in the ODMR spectrum of glassy As_2Se_3 compares favorably with a powder spectrum of the triplet ODMR of the crystal. This fact suggests that the mechanism for midgap luminescence and lattice relaxation in crystals is also present in amorphous samples. The greater degrees of freedom in a disordered sample may lead to metastable configurations which may be responsible for light-induced defects and photodarkening in the amorphous arsenic chalcogenides.

ACKNOWLEDGMENTS

One of us (J.R.) is indebted to the Deutsche Forschungsgemeinschaft for support during which this research was performed. The experiments at the University of Utah were supported by the National Science Foundation under Grant No. DMR-90-47165. The authors thank L. H. Robins for a careful reading of the manuscript and for many helpful suggestions including the possibility of lifetime broadening of the ODMR and the possibility of an Auger recombination process.

[1]B. T. Kolomiets, T. N. Momontova, E. A. Smorgonskaya, and A. A. Babaev, Phys. Status Solidi A **11**, 441 (1972).
[2]N. F. Mott, E. A. Davis, and R. A. Street, Philos. Mag. B **32**, 961 (1975).
[3]M. Kastner, D. Adler, and H. Fritzsche, Phys. Rev. Lett. **37**, 1504 (1976).
[4]J. Ristein and G. Weiser, Solid State Commun. **57**, 639 (1986).
[5]J. Ristein and G. Weiser, Philos. Mag. B **54**, 533 (1986).
[6]J. Ristein and G. Weiser, Philos. Mag. B **56**, 51 (1987).
[7]H. Lundt and G. Weiser, Solid State Commun. **48**, 827 (1983).
[8]L. H. Robins and M. A. Kastner, Philos. Mag. B **50**, 29 (1984).
[9]L. H. Robins and M. A. Kastner, Phys. Rev. B **35**, 2867 (1987).

[10]A. S. Kanishcheva, Yu. N. Mikhailov, E. G. Zhukov, and T. G. Grevtseva, Inorg. Mater. **12**, 1744 (1983).
[11]E. Tarnow, A. Antonelli, and J. D. Joannopoulos, Phys. Rev. B **34**, 4059 (1986).
[12]J. Ristein and G. Weiser, Solid State Commun. **66**, 361 (1988).
[13]J. Cernogora, F. Mollot, and C. Benoît à la Guillaume, Phys. Status Solidi A **15**, 401 (1973).
[14]R. Zallen, M. L. Slade, and A. T. Ward, Phys. Rev. B **3**, 4257 (1971).
[15]H. L. Althaus, G. Weiser, and S. Nagel, Phys. Status Solidi B **87**, 117 (1978).
[16]N. M. Atherton *Electron Spin Resonance; Theory and Applications* (Halsted, New York, 1973).
[17]H. F. Hameka and L. J. Oosterhoff, Mol. Phys. **1**, 358 (1958).
[18]J. W. McIver and H. F. Hameka, J. Chem. Phys. **61**, 825 (1967).
[19]Using λ of 29 cm^{-1} for C, 1550 for As, and 1688 for Se as listed in P. W. Atkins and M. C. R. Symons, *The Structure of Inorganic Radicals* (Elsevier, Amsterdam, 1967).
[20]W. Hayes, M. J. Kane, O. Salminen, R. L. Wood, and S. P. Doherty, J. Phys. C **17**, 2943 (1984).
[21]W. Hayes, Contemp. Phys. **21**, 451 (1980).
[22]R. Zallen and M. L. Slade, Phys. Rev. B **9**, 1627 (1974).
[23]H. L. Althaus and G. Weiser, Phys. Status Solidi B **99**, 537 (1980).
[24]E. Tarnow, M. C. Payne, and J. D. Joannopoulos, Phys. Rev. Lett. **61**, 1772 (1988).
[25]M. Pope and C. Swenberg, *Electronic Processes in Organic Crystals* (Oxford University, New York, 1982).
[26]S. P. Depinna and B. C. Cavenett, Philos. Mag. B **46**, 71 (1982).
[27]A. M. Andriesch and B. T. Kolomiets, Fiz. Tverd. Tela (Leningrad) **6**, 3317 (1964) [Sov. Phys.—Solid State **6**, 2652 (1965)].
[28]G. Brunst and G. Weiser, Philos. Mag. B **51**, 67 (1985).
[29]H. Goldstein, *Classical Mechanics* (Addison-Wesley, London, 1959).